This is an open access article published under an ACS AuthorChoice License, which permits copying and redistribution of the article or any adaptations for non-commercial purposes.

Macromolecules

Perspective

pubs.acs.org/Macromolecules

Approaches to Stretchable Polymer Active Channels for Deformable Transistors

Yujeong Lee,[†] Minkwan Shin,[†] Kaliannan Thiyagarajan,[‡] and Unyong Jeong*[,‡]

[†]Department of Materials Science and Engineering, Yonsei University, 50 Yonsei-Ro, Seodaemun-Gu, Seoul, Korea 120-749

[‡]Department of Materials Science and Engineering, Pohang University of Science and Technology (POSTECH), 77 Cheongam-Ro, Nam-Gu, Pohang, Gyeongbuk, Korea 790-784

ABSTRACT: The fabrication of deformable devices has been explored by interconnecting nonstretchable unit devices with stretchable conductors or by developing stretchable unit devices consisting of all stretchable device components such as electrodes, active channels, and dielectric layers. Most researches have followed the first approach so far, and the researches based on the second approach are at the very beginning stage. This paper discusses the perspectives of the second approach, specifically focusing on the polymer semiconductor channel layers, that is expected to facilitate high density device integration in addition to large area devices including polymer solar cells and light-emitting diodes. Three different routes are suggested as separate sections according to the principles imparting stretchability to polymer semiconductor layers: structural configurations of rigid semiconductors, two-dimensional network structure of semiconductors on elastomer substrates, and ductility enhancement of semiconductor films. Each section includes two subsections divided by the methodological difference. This Perspective ends with discussion on the future works for the routes and the challenges related to other device components.

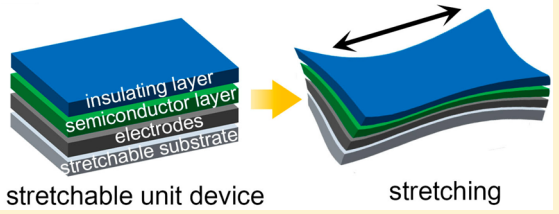

1. INTRODUCTION

Deformable electronics have received great attention during the past decade because new devices are needed beyond the flexible electronics. Currently these electronics include foldable stretchable devices with relatively simple structural designs such as photovoltaics,[1] batteries and capacitors,[2,3] resistive or capacitive tactile sensors,[4−6] and light-emitting diodes.[7,8] Recently, the deformable electronics are extended to active-matrix electronic skins (E-skins) and implanted health care sensors that are expected to replace mechanoreceptors of human beings.[9−12] As described in recent reviews,[13−16] the deformable electronics are expected to advance forward high resolution active-matrix stretchable displays and textile-based wearable devices.[17] To realize the integrated high resolution deformable devices, the unit devices should be operated by transistors, which is a daunting scientific and engineering challenge.

The fabrication of deformable devices has been explored via two different approaches (Figure 1): (I) fabricating conventional nonstretchable unit devices on a rubber substrate or ultrathin film polymer substrate and interconnecting the unit devices with stretchable circuits made of wavy metal lines (Figure 1A); (II) developing stretchable unit devices consisting of stretchable components such as electrodes, active channels, and dielectric layers in addition to the circuits (Figure 1B). So far, most researches on stretchable devices followed the first approach.[18−22] For approach I, the stretchable interconnects on the rubber substrate absorb the stress and stretch selectively along with the rubber substrate. Since the stretchability is imparted by the interconnect, the nonstretchable unit devices are not damaged even at large tensile strains.[21] Recent ultrathin active-matrix

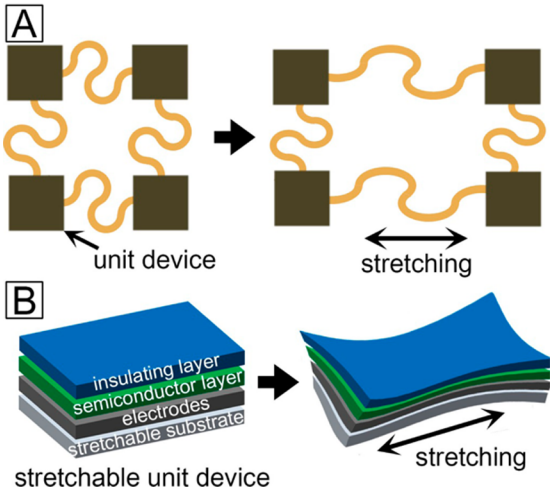

Figure 1. Schematic representation of the different types of stretchable devices. (A) The stretchable serpentine metal lines are connected to the nonstretchable unit devices on a rubber substrate. The stretchability is imparted by the stretchable interconnections (approach I). (B) Stretchable unit device is made up of all stretchable device components, here the substrate, electrode, active, and dielectric layers (approach II).

E-skin devices are also based on a similar concept.[23] The extremely small curvature of the device following the topology of human skin allows stable operation of the device under severe

Received: October 14, 2015
Revised: December 8, 2015
Published: December 24, 2015

Downloaded by POHANG UNIV OF SCIENCE & TECHNOLOGY at 00:19:29:803 on July 01, 2019
from https://pubs.acs.org/doi/10.1021/acs.macromol.5b02268.

© 2015 American Chemical Society

DOI: 10.1021/acs.macromol.5b02268
Macromolecules 2016, 49, 433−444

body motions. The fabrication via approach I is an extension of the conventional device fabrication, which is a great advantage in engineering. But, device density and stretchability are in trade-off because the stretchable metal interconnects and circuits in the approach I require a large space for effective stretching.

Studies on approach II are not established yet. Recent updates are found in some review articles.[24−26] Conventional semiconductors and dielectric layers are solid thin films with a small yield strain, so they are subjected to the formation of cracks or permanent dislocations during repeated bending cycles. Such defects cause the leakage currents in the dielectric layer and a large drop of the charge mobility in the semiconductor. A large tensile strain to dielectrics and semiconductors is expected to cause catastrophic damage on the transistor performance. Therefore, development of stretchable dielectric materials and semiconductors is a big challenge in approach II. There can be a few routes to stretchable semiconductors and dielectrics. Configuring the structure into an appropriate shape to make the systems stretchable is a possible route. Similarly to the wavy metal electrodes, this route allows the hard semiconductors and dielectrics to be stretchable, but the related studies are still rare.[27−29] Development of intrinsically elastic semiconductors and dielectric materials also deserves more studies because such materials can provide ultimate deformability of the device and allow high density integration. A few intrinsically stretchable electronic materials have been attempted such as electrochemical gels for highly stretchable light-emitting[7,30] and two-dimensional (2D) materials for stretchable transistors by relatively small tensile strain (∼5%).[31,32] Rubber composites or electronic materials with a low glass transition temperature (T_g) may be an effective way to make them intrinsically elastic.[24,33−36] A large number of highly stretchable composite conductors have been reported for uses as electrodes and circuits; however, elastic composite semiconductors and dielectrics are at the very initial stage of research.

The term "stretchability" has been used in a fuzzy way without clear definition. Discussion on stretchability needs quantitative mathematical expression. Usually, stretchability (ε_s) is defined as the applied strain (ε_{app}) beyond which the material ruptures or its performance has permanent degradation by a large number of repeated tensile tests. A simple case is a free-standing film, in which the interaction between the film and a rubber substrate can be excluded. The mechanical failure of the free-standing film takes place when the maximum tensile strain (ε_{max}) of the specimen caused by the external strain is equal to the intrinsic critical strain (ε_{cr}) for the material to rupture, $\varepsilon_{max} = \varepsilon_{cr}$.[37] Considering a mechanical stability during a large number of stretching events, one can define the critical strain as the yield strain of the material. When a film is coated on a stretched rubber, the film can accommodate the compressive loading implied by prestrain (ε_{pre}). Prestrain can be included in the stretchability of the film. We often observe that some films fracture catastrophically during repeated stretching even when they accommodate buckles by prestraining. This mechanical failure is related to the maximum bending strain of the film. Therefore, the prestrain for the stretchability should be defined by the maximum strain that the film can endure without any mechanical failure, not by the applied prestrain. Under this assumption, we suggest to define ε_s as follows:

$$\varepsilon_s = \varepsilon_{pre} + \frac{\varepsilon_{cr}}{\varepsilon_{max}/\varepsilon_{app}} \quad (1)$$

This equation indicates that the stretchability can be increased by adding prestrain (ε_{pre}) on the film, by minimizing the value of $\varepsilon_{max}/\varepsilon_{app}$, or by increasing ε_{cr} of the material. It is notable that when a film is subjected to plastic deformation on a rubber substrate, the mechanical behavior is not instant to the external stimulation. A viscoelastic film stretched on a rubber substrate slowly loses the compressive stress by stress relaxation.[38] In this case, the stretchabilty should be defined to involve the stretching frequency, which has not been studied yet. This time-dependent behavior can be important especially in polymer semiconductors because of their low temperature transitions from elastic to plastic deformation. To simplify the concepts of stretchability, we do not consider the time dependency of the film in this Perspective.

On the basis of eq 1, we classified the possible routes to the approach II for achieving high stretchability of polymer semiconductors. The next three sections introduces some recent attempts related to the routes. The structural configuration of rigid semiconductors (section 2) employs the addition of ε_{pre} and the reduction of $\varepsilon_{max}/\varepsilon_{app}$, and the two-dimensional (2D) rubber composites (section 3) are related with the reduction of $\varepsilon_{max}/\varepsilon_{app}$, and the ductility enhancement of polymer films (section 4) increases ε_{cr}. Each section includes two subsections divided by the methodological difference. This paper ends with perspectives discussing the possible opportunities of deformable polymer semiconductors and on the future tasks to achieve.

2. STRUCTURAL CONFIGURATIONS OF RIGID SEMICONDUCTORS

Employing thin layers of rigid electronic materials that are lithographically defined into 2D features is an attractive idea. An advantage of this approach comes from the ability to integrate high-performance material platforms with high engineering control. The device components are well-developed. This approach has successfully used for fabrication of sophisticated electrodes but not much for semiconductors. This section covers the principles of structural semiconductor configurations to attain stretchability.

2.1. Out-of-Plane Wavy Structure Using Prestrain (ε_{pre}).

A rigid semiconductor film placed on a prestrained elastomer substrate undergoes a compressive force in the lateral direction after the prestrain on the rubber substrate is released. When the adhesion between the semiconductor film and the rubber substrate is strong enough, the film forms the out-of-plane sinusoidal wrinkle structure.[39] Figure 2A illustrates the prestrain strategy in a semiconductor film on a rubber substrate. When the film is fully stretched, ε_{app} is equal to ε_{max}; therefore, the stretchability is usually determined by the prestrain of the substrate.[37] In the out-of-plane sinusoidal structure without prestrain, the stretchability is expressed as $\varepsilon_s = (L_{max} - L_0)/L_0$, where $L_{max} = 2N\int_0^{\pi}[1 + ((2\pi A/\lambda)\cos(2\pi x/\lambda))^2\,dx]^{1/2}$ with an amplitude (A) and wavelength (λ).[40] The wavelength and amplitude are governed by the moduli of the film (E_f) and substrate (E_s), the thickness (h_f) of the film, and prestrain (ε_{pre}). Since Rogers and co-workers demonstrated the highly stretchable devices using the wrinkled Si nanoribbons,[41] many researchers have utilized the process in a wide range of applications.[18−22,42,43] Recently, Bettinger and co-workers used the buckles to fabricate large-area stretchable organic thin film transistors that can operate under strains up to 12%.[44] They examined two source/drain electrodes configurations that are parallel and perpendicular to the grooves (Figure 2B). Devices fabricated on the topographic substrates exhibited stable

DOI: 10.1021/acs.macromol.5b02268
Macromolecules 2016, 49, 433−444

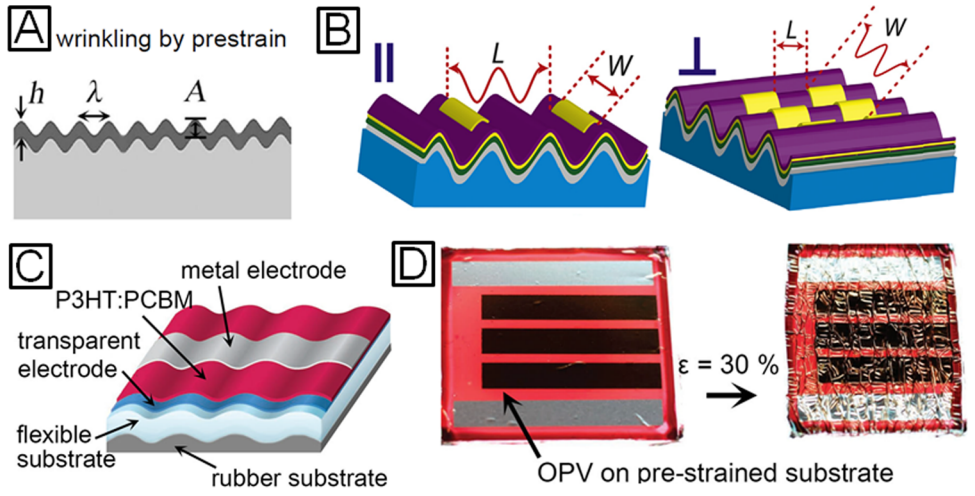

Figure 2. (A) Schematic illustration of the wrinkle generation in a semiconductor layer on a rubber substrate by applying the prestrain to the rubber substrate. λ, A, and h denote wavelength, amplitude, and film thickness, respectively. (B) Stretchable device configurations of organic thin film transistors fabricated on a wrinkled rubber substrate. The source/drain electrodes are arranged parallel and perpendicular to the topographic features. Figure adapted with permission from ref 44. (C, D) Schematic diagram of the ultralight, deformable organic solar cell (C), and an ultrathin solar cell (D). The solar cell was fabricated on a prestrained rubber substrate (left), where the device under compressive force is shown at 30% compressive strains after the prestrain was releasd. Figure adapted with permission from ref 45.

operation with maintaining high mobilities and on−off ratios compared to the devices fabricated on flat substrates. The saturation mobility gradually decreased as the strain was increased to 12% in both the configurations, but it showed the possibility of stretchable transistors on the periodic grooves.

Currently, most studies taking advantage of this out-of-plane configuration have been the fabrication of stretchable organic photovoltaics (OPVs).[1,45,46] Stretchable OPVs can draw new possibilities of portable devices that can be folded and installed on the surfaces with complicated curvatures and human bodies with large stretching motions. Bao and co-workers demonstrated the first stretchable OPVs on a prestrained rubber substrate.[1] The out-of-plane wrinkle structure of the bulk heterojunction layer imparted the stretchability on the solar cells. They used PEDOT:PSS as the electrode and liquid metal contacts for the device interface. Another example was accomplished by Someya and co-workers.[45] They fabricated an OPV on a ultrathin poly(ethylene terephthalate) (PET) substrate and then transferred it onto a prestrained rubber substrate (Figure 2C). Again, the wrinkles of the OPV allowed high stretchability (up to 50% tensile strain) and foldability (Figure 2D). The stretchable performance should be investigated further because power conversion efficiencies of OPVs using PEDOT:PSS are still inferior to those of OPVs using ITO electrodes. Very recently, Lee and co-workers succeeded to prepare highly conductive PEDOT:PSS with conductivity more than 4000 S/cm, and they achieved power conversion efficiency of 6.6% that is nearly comparable to the value from the ITO-based OPVs.[46]

Unfortunately, the large-area wrinkle causes the structural colors from the periodic sinusoidal structure.[47] Localized out-of-plane sinusoidal structures in unit devices and their connection to intrinsically stretchable interconnections may remove the structural colors; it may also realize simultaneous achievement of high device density and high stretchability. A few processes have been developed for generating localized wrinkle patterns in a continuous thin film, including stamp-mediated patterning of localized wrinkles,[48−50] local air expansion-induced wrinkles,[51] and local heating-induced wrinkles. Transfer of a patterned semiconductor channel on a prestrained rubber can be another approach to impart stretchability and high resolution.[52]

2.2. In-Plane Wavy Structure Minimizing the Maximum Tensile Strain (ε_{max}). In-plane serpentine patterns fabricated on rubber substrates are well established.[37,53−58] Figure 3A shows

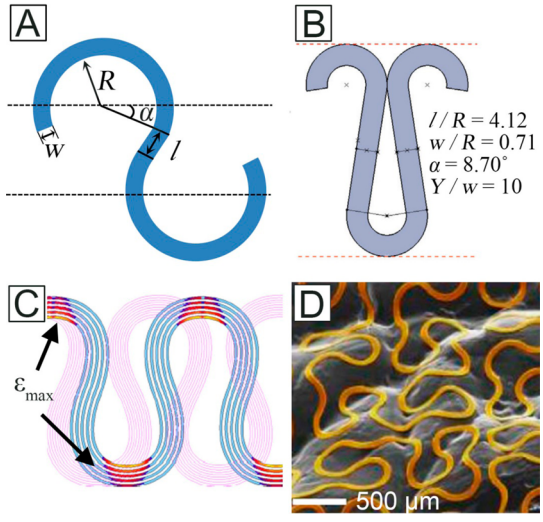

Figure 3. (A) Schematic representation of a serpentine unit cell where w, R, α, and l are the width, the radius of the arc, the arc angle, and the arm length of the serpentine unit, respectively. Figure adapted with permission from ref 37. (B) The shape of the serpentine under the practical constraints (X = 0 and Y = 10w). Figure adapted with permission from ref 37. (C) Structure and strain distribution of the multiserpentine trace. Figure adapted with permission from ref 54. (D) Colored scanning electron microscopy image of the fractal structured electrode. Figure adapted with permission from ref 58.

the unit cell of a generic serpentine that is defined by four geometric parameters of the pattern: the width (w), the arc radius (R), the arc angle (α), and the arm length (l). The thickness of the pattern is usually not taken into consideration in the plane strain mode. In this planar configuration, the stretchability is

DOI: 10.1021/acs.macromol.5b02268
Macromolecules 2016, 49, 433−444

governed by the four parameters because the dimensionless parameter is a generic function for linear elastic materials, $\varepsilon_{max}/\varepsilon_{app} = f(\alpha, w/R, l/R)$. The analytical functional form is complicated, so it is not easy to tell the pure effects of the three variables. In general, the stretchability increases with small w/R, large l/R, and large α.[54] For a simple but frequently observed case, $l = 0$ and $\alpha = 0°$, the dimensionless parameter is simplified, $\varepsilon_{max}/\varepsilon_{app} = (4/\pi)(w/R)(2 - w/R)^{-1}$.[37] When $w/R \ll 1$, the dimensionless parameter becomes more intuitive, $\varepsilon_{max}/\varepsilon_{app} \approx (2/\pi)(w/R)$. From eq 1, the stretchability can be 15% when $w/R = 0.1$ and $\varepsilon_{cr} = 1\%$ (for example, a pattern with 3 μm width and 30 μm arc radius). Narrower serpentines (smaller w) can provide more stretchability. In practical circuit design, the design of the serpentine structure is subjected to fabrication constraints. Practically accessible minimum width is predetermined (typically a few micrometers) and the breadth (Y) of the serpentine ranges $5w-15w$, and the serpentine do not overlap ($X \geq 0$).[7] With the constraint $Y = 10w$, the optimal design for the minimal value of $\varepsilon_{max}/\varepsilon_{app}$ is determined as $\alpha = 8.7°$, $w/R = 0.71$, and $l/R = 4.12$ (Figure 3B).[7] By a predetermined minimum width in fabrication, the other dimensions are determined. It is notable that ε_{max} is strongly dependent on the adhesion with the rubber substrate. Strong adhesion can greatly reduce ε_{max}, so increasing the stretchability. There have been many researches on stretchable electrodes to minimize ε_{max} at high values of tensile strain (for example, $\varepsilon_{app} = \sim 50\%$).[37,53−58] Since conventional semiconductors in FETs are solid thin films, the strategies for stretchable semiconductors may have clues from those for the stretchable electrodes.

A semiconductor pattern with a single-line serpentine is disadvantageous in the channel width. Increasing the width (w) can improve the device performance, but it reduces the stretchability. Increasing the amplitude can reduce the accumulated strain, but it is not desirable for high density device integration. Subdividing the serpentine line in several lines of smaller width can reduce more strains without sacrificing the electrical performance or changing the amplitude (Figure 3C). The stretchability of this multiserpentine trace with w_0 improves the stretachability more than a single serpentine trace with the same w_0,[54] which may enable to achieve both high stretchability and high device performance. This multiserpentine trace is also advantageous in prevention of sudden crack propagation in the serpentine. The cracks in the single serpentine result in abrupt failure of the device, whereas the rubber between the serpentines of a multiserpentine trace plays as a buffer to block the propagation of the cracks.[54,59] Two-dimensional (2D) serpentine layouts may also be useful especially to the devices that are stretchable in biaxial directions.[57] One-dimensional (1D) serpentine is weak to the tensile stress along the perpendicular direction to the serpentine direction. Recently 2D fractal structures were suggested for highly deformable electrodes in any tensile direction (Figure 3D).[58] Such structure may be another approach to attain biaxially deformable semiconductors if the width of the semiconductor fractal line is small for high density device integration.

So far, there has been no report that utilized the serpentine structure to create an active channel of a semiconductor. This is partly because the serpentine structures of the brittle inorganic semiconductors are less effective in obtaining large stretchability. The stress accumulated in the serpentines may alter considerably the channel performance. And the other reason is that the current serpentine strutures are too large for high performance semiconductor channels. In order to achieve both the large stretchability and high performance, the width of the serpentines should be reduced greatly (probably in the level of 1 μm) with excellent adhesion with the elastomer substrates. Decreasing the thickness of the channel layer can be another approach to enhanced flexibility of the structure; hence, the 2D semiconductors such as transition metal chalcogenides (MoS_2, WS_2, $MoSe_2$, WSe_2, etc.) are good material candidates for this approach.[60−63] Currently, the synthesis of the 2D material thin films in large area (in wafer scale) is a challenging task to be achieved.

3. TWO-DIMENSIONAL NETWORK STRUCTURE ON ELASTOMER SUBSTRATES

In the approach of structural configuration discussed in section 2, the charges transport along the curved lines with feature sizes larger than a few micrometers. Film-type semiconductor channel layers are more desirable for the fabrication of high-density field-effect transistors. Dynamic cross-links between the synthetic polymers by hydrogen bonds, metal−ligand coordination complex can facilitate responsive mechanical properties.[64] Recently, a few approaches were suggested to obtain stretchable semiconductor films. The approaches covered in this section attempt to produce a network of 2D electrical percolation formed on an elastic substrate.

3.1. Semiconductor Nanofibril Network Film Indented in an Elastomer Substrate. When a tensile load is applied to a thin film constructed with nanofibrils, the potential energy (E) of the film is a sum of the energy contributions from the nanofibrils, $E = E_{stretch} + E_{bend} + E_{vdw}$.[65] Since the interfibril interaction energy (E_{vdw}) is the weakest among the three energies, the initial load is mostly carried by E_{vdw}. Figure 4A shows simulation results of a

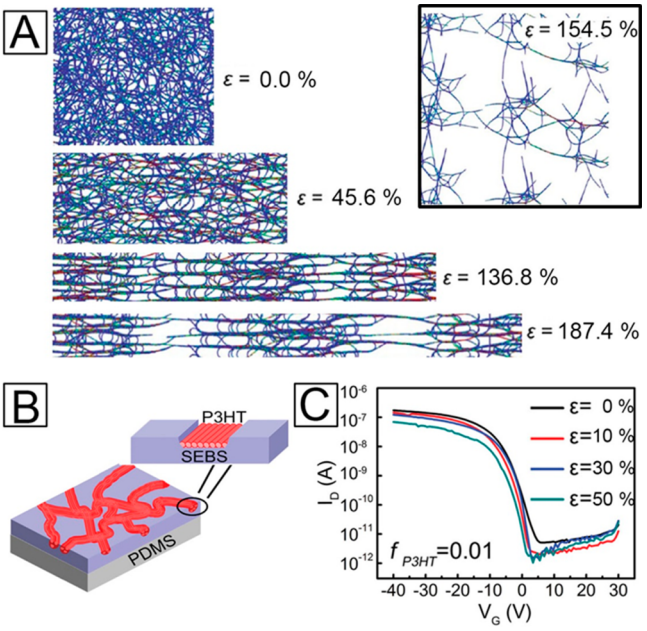

Figure 4. (A) Structural changes of the carbon nanotube networks under different levels of tensile strain. Here, the different color indicates the stress levels in the CNT network. Blue color represents zero or compressive stress, while the red color corresponds to maximum stress. The inset represents a structural change under biaxial elongation. Figure adapted with permission from ref 65. (B) Schematic illustration of the stretchable P3HT nanofibril network (active channel layer) on the SEBS rubber surface and (C) transfer curve of the nanofibril field effect transistor at different tensile strains. (B) and (C) adapted with permission from ref 59.

DOI: 10.1021/acs.macromol.5b02268
Macromolecules 2016, 49, 433−444

CNT network under uniaxial elongation.[65] As the strain increases, the film experiences considerable shrinkage in the transverse direction and the nanofibrils tend to align through rotation and sliding. At a certain level of tensile load, the overall distance between the nanofibrils becomes small enough to form bundles. The strain-induced alignment leads to the formation of thick bundles of the nanofibrils.[65,66] The thick nanofibril bundles have enhanced rigidity that is proportional to the diameter of the bundles, so they maintain a network of the bundles at higher tensile strains. Deformation of the network along the tensile direction leads to apparent stretching of the thin film even when the network filaments are not stretchable. At large strains, the bundles are separated into several blocks with relatively smaller deformation within the blocks, and then the bundles interconnecting the blocks are pulled out to cause mechanical failure of the nanofibril film.[65−70] Once this plastic deformation takes place, the microstructure is irreversible.

On the basis of the failure mechanism described above, mechanical stability of the nanofibril film at high tensile strains can be improved by several ways. First, restricting the viscoelastic behavior of the nanofibrils such as sliding, rotating, and pulling-out can enhance mechanical stability of the nanofibril film at high tensile strains. When the nanofibrils are embedded or indented in an elastic medium having strong adhesion, the mechanical deformation of the nanofibrils is affined until the tensile load is comparable to the potential energy for stretching ($E_{stretch}$).[66] When the semiconductor layer is to be used in a field effect transistor, indentation of the semiconductor nanofibrils in the top surface of the rubber substrate is more desirable to make effective contacts with source (S) and drain (D) electrodes. The mechanical stability can be enhanced also by cross-linking the nanofibrils instead of relying on the weak molecular interactions. Since the damping factor (ξ) of a network is inversely proportional to the strength (k) of the cross-linked network ($\xi \propto 1/k^{1/2}$), strong cross-links prevent the plastic deformation of the nanofibril films. The pore size of the nanofibril network is another critical parameter for stretchability. To attain high channel performance and reliability of the semiconductor layer, surface coverage of the nanofibrils should be large, but it is not favorable for high stretchability because of the small pore size. Bundling of the nanofibrils may be a good solution for this issue. Repeated tensile stretching of the nanofibril film leads to a bundle network with larger pores.

This nanofibril network has been used to produce stretchable transparent electrodes. Improved adhesion between rubber substrate and a network of 1D nanomaterials could provide high conductivity and stretchability.[26] Various coating processes are available, such as spin-coating, spray-deposition, bar-coating, or screen printing. The electrical conduction was improved by adding binders and surfactants[7,71] or forming hybrid structures with graphene oxide, CNT, and graphene.[26,72] Very recently, Jeong and co-workers utilized this approach to demonstrate a stretchable polymer semiconductor network film.[59] Conjugated semiconducting polymers have typically poor miscibility with other polymers because of their strong assembly into $\pi-\pi$ stacked directional crystals.[73] They took advantage of the phase separation between poly(3-hexylthiophene) (P3HT) and poly(styrene-*b*-ethylenebutadiene-*b*-styrene) (SEBS) during spin-coating. P3HT formed a nanofibril network film on the top surface of the SEBS layer because of the low surface energy of P3HT. The P3HT nanofibrils were indented in the SEBS rubber surface but exposed to the air, which facilitated the use of the nanofibril network as a channel layer (Figure 4B). Once the nanofibrils were formed, they self-organized into nanobelt-like bundles. This multiserpentine structure in nanoscale enabled high stretchability without losing electrical conduction, as described in section 2.2.[65,66] The network thin film showed stable transistor performance during repeated stretching tests at 50% tensile strain with small change of mobility and on−off ratio.[59]

3.2. Microcrack Formation in Semiconductor Films.

The formation of cracks in a thin film is generally considered deleterious. But, microcracking in a film may lead to improved toughness.[74] Here is a scenario desirable for high tensile endurance of a semiconductor film. A film begins to crack at a critical stress, and the stress−strain curve becomes nonlinear which is due to the combination of compliance increase and dilatational strain around the microcracks. If the material is unloaded prior to mechanical failure of the film, the microcracks remains opened. If the microcracks are stable so they grow very slowly, repeated cycles of loading and unloading causes the generation of new microcracks.[75] In the end, the film will form a network of ligaments of the semiconductor film. This microcrack formation increases the mechanical stability of the film to tensile strains; also, it can maintain the electrical percolation through the network of the film ligaments.[76−79] This scenario is not usually acceptable for a brittle solid film on a solid substrate because the microcracks are not stable; hence they grow rapidly. But, the scenario may be applied to a ductile film on an elastic substrate. Lacour and co-workers observed that a thin Au film on an elastomer substrate can deform elastically under large tensile strain without forming plastic deformation.[76] Finite and reproducible electrical conduction was maintained over repeated tensile tests. The microcracks in the Au film were elongated by deflecting and twisting out of plane (Figure 5A). The out-of-plane deformation resulting from the highly compliant elastomer substrate minimized the energy released at the crack tips; hence, the microcracks were stable enough not to grow across the metal film.[76]

Typical polymer semiconductors have lower moduli than those of metals, and their films have comparable ductility with those of metal films.[80] These relatively ductile property of polymer semiconductors can be used for microcrack-assisted stretchable semiconductor thin films. Bao and co-workers investigated the formation of microcracks generated in P3HT films.[81] When a P3HT thin film was transferred onto a polyurethane (PU) substrate, macroscale cracking took place below 15% tensile strain, and the crack width continued to increase to the level of 10 μm (Figure 5B). Meanwhile, when a P3HT was directly spin-coated on a PU substrate, onset of observable microcracks occurred at about 50% strain, and the crack width was limited in micrometer scale even at 200% strain (Figure 5C). The polymer chains in the film with the microcracks were aligned in the direction of stretching (investigated by dichroic ratio), whereas the chains in the macroscale cracks showed negligible alignment. This result is attributed to the enhanced adhesion between the P3HT film and the PU substrate, which improves ductility of the P3HT chains by limiting the localization of strain that is responsible for the large-scale crack formation.[82−84] Similar microstructural development was observed when a thin PU film was placed on the P3HT film spin-coated on the PU substrate. Using the upper PU film as the gate dielectric layer, the gate effect of the P3HT film was investigated under repeated 40% strain (Figure 5D). Device performance showed degradation in both the perpendicular and parallel directions to the stretching (Figure 5E),[81] but the gate effect of the P3HT layer was preserved. Similar results were reported in pentacene devices.[85] O'Connor et al. reported that

DOI: 10.1021/acs.macromol.5b02268
Macromolecules 2016, 49, 433−444

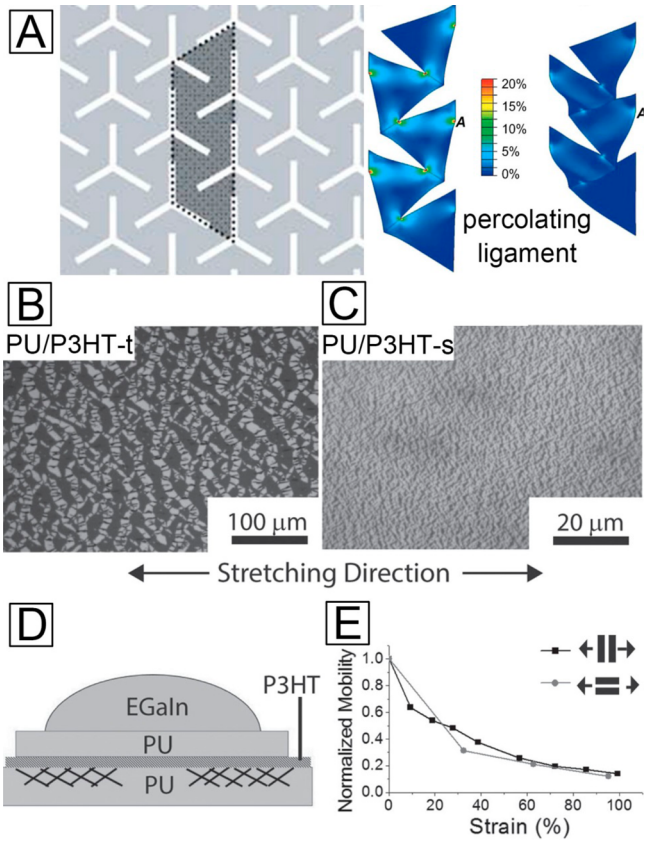

Figure 5. (A) Schematic model of tribranched cracks in a thin film (left) and the simulation result of the model (right). The color indicates the strain accumulated in the percolating ligament. Figure adapted with permission from ref 75. (B, C) Effect of the strain on the structure and morphology of the P3HT film on the PU surface. P3HT film was transferred on the rubber (B) and directly spin-coated on the rubber (C). (D, E) Schematic of the top-gated field effect transistor where the stretchable P3HT is used as the active channel layer (D) and its normalized mobility change under biaxial tensile deformation (E). (B)−(E) adapted with permission from ref 81.

the mobility of P3HT increased perpendicular direction but decreased in the parallel direction.[83] The crack formation and failure mechanisms should be investigated in more details for various device setups.

4. ENHANCING DUCTILITY OF POLYMER FILMS

Compared with inorganic semiconductor thin films, polymer semiconductor thin films are more compliant to flexible electronics and applicable to continuous roll-to-roll manufacturing process. From the literature data, mechanical flexibility of polymer semiconductors is highly variable.[80,86−88] Stiffness of polymer semiconductor thin films increases with high degree of crystallinity and long conjugation length, which is unfortunate because such stiff semiconductors show better electronic performance but less stretchable. If the ductility of the polymer semiconductor thin films is improved without degrading their electronic performance, it will be a promising approach to enhance stretchability of the polymer thin films. This section introduces design of molecular structures and addition of plasticizers to obtain high ductility of semiconducting polymer thin films.

4.1. Control of Molecular Structures. The sp^2-hybridized highly conjugated polymer main chains give rise to the electronic band structure at the expense of conformational freedom. The $\pi-\pi$ interaction between the conjugated backbones due to their high polarizabilty is another contribution to the chain rigidity.[89−91] Recent studies reveal that the length of alkyl side chains attached to the polythiophene backbones in poly(3-alkylthiophene) (P3AT) plays a critical role in reduction of the rigidity of their thin films.[88,91] Lipomi and co-workers have made large attention to this issue. Details are summarized in their recent review article.[77] The reduced volume fraction (v_f) occupied by the polythiophene backbone chain is the main reason for the rigidity decrease; $v_f = 0.31$ for butyl side chains, and $v_f = 0.20$ for dodecyl chains. The glass transition temperature (T_g) of P3HT is known to be near room temperature (~20 °C),[92,93] while the T_gs (<0 °C) of poly(3-heptylthiophene) (P3HpT) and poly(3-octylthiophene) (P3OT) are substantially below room temperature (Figure 6A).[88,91] Seitz et al. reported a semiempirical theory predicting the modulus of simple conjugated polymers.[94] The tensile modulus (E_f) of a thin film is related to the bulk modulus (B) and the Poisson ratio (ν), $E_f = 3B(1 - 2\nu)$. The bulk modulus is related to the cohesive energy (E_{coh}), the van der Waals volume (V_w), and the molar volume (V) at a temperature (T), $B \approx 8.23E_{coh}[(5V_0^4/V^5) - (3V_0^2/V^{35})]$.[94] The cohesive energy is calculated from semi-empirical parameters derived from the bond connectivity indices in a method described by Fedors.[95] The Poisson ratio is related to the cross-sectional area (A) of the monomer, $\nu = 0.513 - 2.37 \times 10^6\sqrt{A}$, and the area is determined, $A = V_w/(N_A l_m)$, where l_m is the length of the monomer. Prediction of the tensile modulus based on the empirical equation is consistent with measured values.[91] The tensile modulus of P3HT is typically ~1 GPa which causes cracks at low tensile strains (<2.5%); meanwhile, the tensile moduli of P3HpT and P3OT substantially decrease to ~0.1 GPa. Further increase of the length of the alkyl side chains does not result in further decrease of the tensile modulus.

Decrease of the tensile modulus should be accompanied by high device performance. So far, the correlation between the stretchability of polymer semiconductors and their device performance is rarely investigated. Very recently, Lipomi and co-workers studied a series of P3AT to find an optimal semiconducting polymer which is valuable for high stretchability without the loss of device performance.[88,96] Unfortunately, severe degradation of the hole mobility was measured in P3HpT and P3OT (Figure 6B). Since the injection barriers at Au/P3AT interface are small, the performance degradation is attributed to the structural difference of the semiconducting polymers. But, they found that P3HpT:PCBM mixture can increase the hole mobility of the polymer, so the power conversion efficiency of the bulk heterojunction solar cell was comparable to the value of P3HT:PCBM combination (Figure 6B).[80,96] Although the tensile modulus of the mixture film increased with the increasing wt % of PCBM, the P3HpT:PCBM solar cell showed enhanced stretchability compared to the P3HT:PCBM solar cell. This molecular structure control should be studied for various types of semiconducting polymers, especially for high mobility polymers. The active channels for solar cells should be accompanied by the development of flexible n-type materials instead of PCBM.[97]

A more progressive work was conducted by Qiu and co-workers.[98] They synthesized polythiophene-*b*-rubber-*b*-polythiophene (P3HT-*b*-PMA-*b*-P3HT) triblock copolymer to obtain the thermoplastic elasticity. The triblock copolymer self-assembled into a well-ordered nanofibrillar structure by thermal annealing (Figure 6C). The elasticity was derived from the rubbery matrix poly(methyl acrylate) (PMA) and the hard

DOI: 10.1021/acs.macromol.5b02268
Macromolecules 2016, 49, 433−444

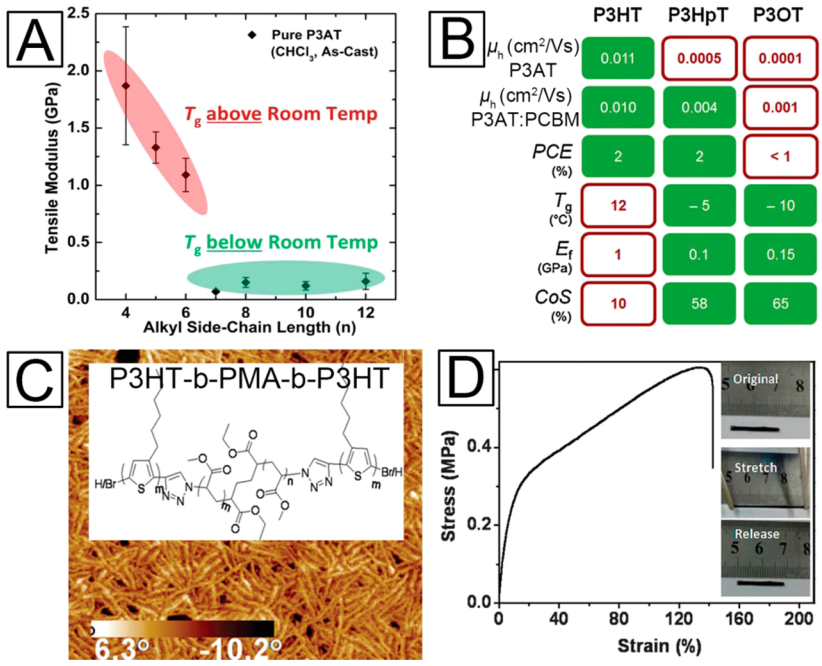

Figure 6. (A) Comparison of the tensile modulus of the P3AT at glass transition temperature (T_g) above and below room temperature. Figure adapted with permission from ref 91. (B) Electronic and mechanical properties of P3HT and P3HpT and its polymer:fullerene blends. The favorable and unfavorable properties are indicated in green and red, respectively. Figure adapted with permission from ref 96. (C) AFM topography image of P3HT-*b*-PMA-*b*-P3HT triblock copolymer shows the nanofibrillar structures. The inset is the chemical structure of the triblock copolymer. (D) The stress–strain curve of the triblock copolymer. (C) and (D) adapted with permission from ref 98.

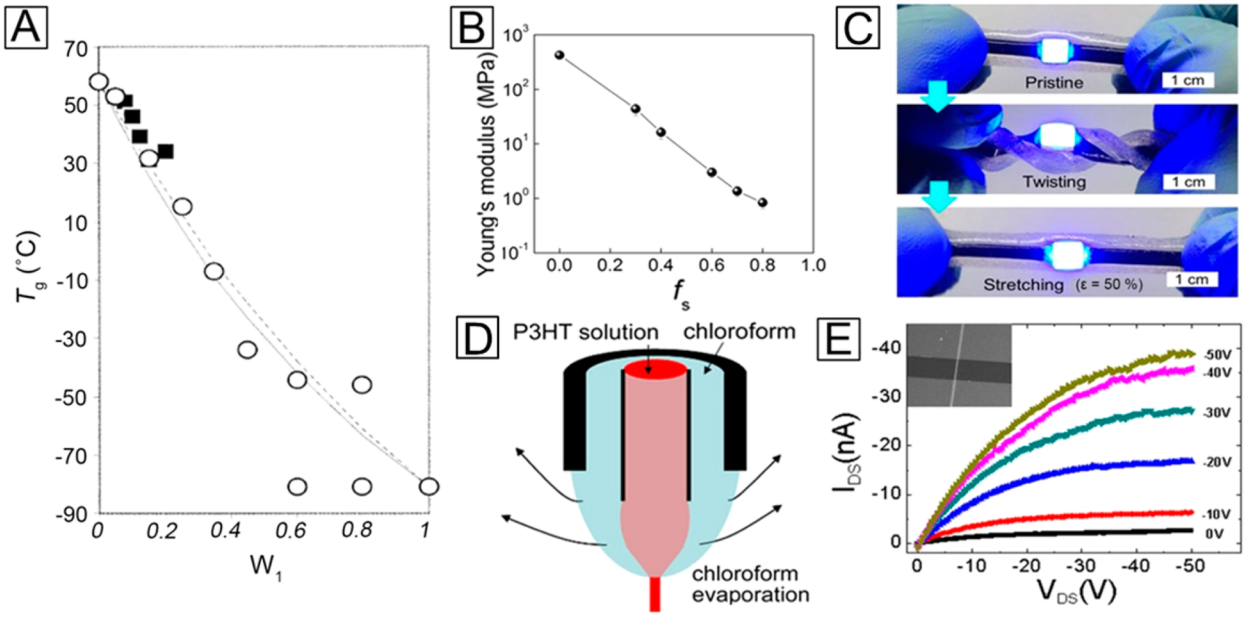

Figure 7. (A) Glass transition temperature (T_g) of poly(L-lactic acid) as a function of a plasticizer (ATBC) weight fraction (W_1). The hollow circle (○) indicates the solution cast and the solid square (■) represents the melt-blended and injection-molded sample. The lines present theoretical predictions: dotted line with the Fox equation and solid line with the Couchman–Karasz equation. Figure adapted with permission from ref 100. (B, C) Young's modulus of plasticized PEDOT:PSS as a function of the surfactant weight fraction (f_s) and a demonstration of a deformable LED fabricated on the plasticized PEDOT:PSS circuit. Figures adapted with permission from ref 108. (D) Schematic description of coaxial electrospinning setup, the P3HT/PCL mixture solution is fed through the inner nozzle, and a small amount of pure chloroform is provided to retard the evaporation of the solvent. (E) The channel current vs drain-source voltage (I_{DS}–V_{DS}) characteristics of the pure P3HT/PCL mixture nanofibers FET. (D) and (E) adapted with permission from ref 110.

nanofibril microdomains, which is typical in block copolymer-based thermoplastic elastomers. It showed an elastic behavior with a small Young's modulus (6 MPa) and a large elongation at break (140%) (Figure 6D). Although the charge mobility is far inferior to the industrial standard, semiconductor–rubber block copolymer systems would provide a powerful platform for the preparation of semiconducting polymers with intrinsic stretchability.

DOI: 10.1021/acs.macromol.5b02268
Macromolecules 2016, 49, 433–444

4.2. Addition of Plasticizers. Plasticization of polymers with additives has been commonly used in polymer processing.[99,100] The additives can be small molecules with high boiling points, oligomers, and polymers with a low T_g. The primary role of a plasticizer is to reduce glass transition temperature (T_g) of the polymer by increasing the free volume; hence, the tensile modulus decreases. T_g of a plasticizer-containing polymer mixture can be estimated by a simple equation proposed by Fox[101]

$$\frac{1}{T_g} = \frac{w_1}{T_{g1}} + \frac{w_2}{T_{g2}} \tag{2}$$

where subscripts 1 and 2 refer to plasticizer and polymer, respectively, and w is the weight fraction up to the solubility limit. The simple equation has been used to estimate the change of T_g of crystalline polymers and proved consistent with experimental results. Figure 7A shows the change of T_g of poly(L-lactic acid), a crystalline polymer, as a function of the weight fraction (w_1) of a plasticizer, acetyl tributyl citrate (ATBC). From the experimental results and the Fox equation, T_g of the mixture is inversely proportional to the weight fraction of the plasticizer. For example, T_g of P3HT (~20 °C) may be reduced to ~−5 °C at w_1 = 0.2 provided the plasticizer (T_g = −60 °C) is miscible with P3HT. Since the tensile compliance becomes prominent when the T_g of a polymer is below room temperature, the change of T_g can result in considerable decrease of the tensile modulus.

Very recently, the plasticization of PEDOT:PSS has been attracting much interest because the enhanced compliance of the plasticized PEDOT:PSS showed a considerable degree of flexibility and the possibility of stretchable electrodes.[1,102−107] Addition of high-boiling liquids such as sorbitol,[102] dimethyl sulfoxide (DMSO),[103] Zonyl fluorosurfactant,[1,104] nonionic surfactant (Triton X-100),[105] and amine-containing polymers[106,107] are known to enhance both the conductivity and flexibility of the PEDOT:PSS. Very recently, Jeong and co-workers demonstrated that addition of a large amount (~70 wt %) of surfactant (Triton X-100) in the PEDOT:PSS/surfactant mixture reduced greatly the Young's modulus (Figure 7B) and imparted a 10% stretchability to a free-standing film and a 50% stretchability to a film coated on a rubber substrate (Figure 7C).[108] The play-dough-like viscoelastic property of the plasticized PEDOT:PSS allows molding of the PEDOT:PSS into various microstructures by simply pressing a PDMS stamp on the PEDOT:PSS thin film.

So far, plasticization of semiconducting polymers has not been studied actively. It is because plasticization is expected to cause considerable decrease of charge mobility, which is contrast to the enhanced conductivity in the plastisized PEDOT:PSS.[102−108] Still there has been no report to disprove this antithetical relationship[109] between the electronic performance and the mechanical compliance of semiconductors. But, recent studies on the elastic polythiophene/rubber composites report that the charge-carrier mobilities of the composites showed mobilities comparable to the values of their continuous thin film counterparts.[59] The enhanced mobility along the high quality nanofibrils of the polythiophenes is the main contribution to the preservation of the charge mobility. This concept may be utilized in the addition of plasticizing polymers (low-T_g polymers). Phase separation between the plasticizing polymer (A) and polymer semiconductors (B), forming minor domains of the plasticizer in a continuous semiconductor matrix, may reduce the tensile moduli of their thin films. Previous study based on the electrospinning of a mixture solution of P3HT and poly(ε-carprolactone) (PCL) showed that the charge-carrier mobility is degraded by only 1 order (from 0.017 to 0.012 $cm^2/(V\,s)$) even when PCL was mixed by 20 wt % (Figure 7D,E).[110] The other P3HT fiber-based works showed reasonable device performances.[111,112] Takanogi derived a mathematical model as an aid to understanding the viscoelastic behavior of a binary polymer blend in terms of the properties of the individual components.[113] If the volume occupied by the interface between the domain phase and the matrix phase is negligible, the modulus of the composite (E_c) is predicted by Takayanagi's equation

$$E_c = \lambda\left(\frac{\varphi}{E_A} + \frac{1-\varphi}{E_B}\right)^{-1} + (1-\lambda)E_B \tag{3}$$

where E_A and E_B are the Young's modulus of the plasticizer (A) and the semiconductor domain (B); λ and φ are the volume fraction of domain phase and the volume fraction of the plasticizer in the domain phase. The volume fraction of the plasticizer (v_A) in the composite is thus $v_A = \lambda\varphi$. If the domain phase consists of the pure plasticizer ($\varphi = 1$), which is reasonable because solubility of semiconducting polymers in the plasticizer phase is not high, Takayanagi's equation is simplified by their volume fractions of the plasticizer (A) and semiconductor (B)[114]

$$E_c = \lambda\varphi E_A + (1-\lambda)E_B = v_A E_A + v_B E_B \tag{4}$$

In order to describe mixtures of crystalline polymer matrix, Gray and McCrum proposed an empirical logarithmic mixing rule[115]

$$\log G_c = v_A \log G_A + v_B \log G_B \tag{5}$$

In both equations, the modulus of a polymer composite is sensitively dependent on the volume fraction of the plasticizer.

5. PERSPECTIVES

The routes introduced in this article for obtaining stretchable polymer semiconductors are in their very initial stages or have not been explored yet. Each route has challenging engineering hurdles to be overcome. The out-of-plane approach requests prestrain of the rubber substrate, which is not appropriate to current printed electronics. The buckling induced by the large modulus difference between the rubber substrate and the top layer can cause severe stress in the channel layer during the repeated tensile stretching. Localized buckling of the unit devices looks more desirable instead of buckling over a large-size film. It may remove the structural colors reflecting from the large-area buckles and allow direct printing of polymer semiconductors on the rubber substrates. The serpentine configuration needs high density coverage of the semiconductor pattern to obtain high performance channel layer. The crack formation and its propagation in the semiconductor line patterns should be studied in a systematic way because the microstructures in polymer thin films vary sensitively by the coating conditions and molecular structures. Prediction of the mechanical behaviors of the polymer serpentine lines is more complicated compared to the metal lines. So far, the 2D percolating networks made of nanofibrils or microcracked ligaments showed possibilities of stretchable semiconducting polymer films. In the nanofibril network, the dimensions of the nanofibrils and their areal density in the film should be uniform. In use of metal nanowires or CNTs, the presynthesized materials are uniformly dispersed in the solution and deposited on the substrate without changing their initial structures; hence, the concentration is the governing parameter in the uniformity of their films. When polymer solutions are

DOI: 10.1021/acs.macromol.5b02268
Macromolecules 2016, 49, 433−444

coated, the nanofibrils *in situ* grow during the coating process, so the dimensions of the resulting nanofibrils depend on the coating conditions. Although direct coating of uniform polythiophene nanofibrils has been reported,[116−118] polymers with better charge mobilities should be produced in uniform nanofibrils. In the microcrack approach, reliability under severe tensile conditions should be confirmed, and the size of the microcracks needs fine control for reproducible device performance. A few recent studies attempted to control the propagation of microcracks in thin films,[119,120] but more experimental and theoretical studies are needed to suggest optimal morphologies of the microcracked thin films for the use as channel layers. Highly ductile semiconductors are advantageous in that they can be immediately applied to current printed electronics. The ductile characteristic provides good adhesion to the device components such as substrates, electrodes, and dielectric layers. However, achieving ductility without losing the channel performance is a challenging task. Ductility is a function of temperature. Even polythiophenes with long alkyl chains such as P3HpT and P3OT are brittle at below 0 °C. Synthesis of a rubber-like semiconductor with a T_g far lower than 0 °C is desirable. Block copolymers with a continuous network of semiconducting microdomains in a viscoelastic matrix are attractive materials. Addition of plasticizers decreases the charge mobility as the volume fraction of the plasticizer increases. The plasticizers can also change the work functions of the metals and semiconductors. Current status of this approach lacks guidelines about choosing proper plasticizers for semiconducting polymers of interest.

In all the routes discussed above, strong interlayer adhesion is important. Specific adhesions between the semiconducting polymer phase and the rubber or additive phase, such as hydrogen bonding and chemical cross-linking, considerably improve the mechanical and electrical stabilities. The atmospheric plasma deposition process investigated by Dauskardt and co-workers may be a promising way to prepare multilayers with strong adhesion in a relatively inexpensive way over a large area.[121−123] To provide correct information on the device characteristics, testing device performance needs standardized procedure. Stretchability of polymers can be sensitive to temperature (especially at low temperatures for polymer semiconductors). Stability in a cyclic change of temperature should be tested in addition to the mechanical tests at room temperature because the rubber substrate of the deformable devices are subjected to repeated thermal expansion and contraction. The real strain in the measurement area should be provided for proper analysis on the effect of deformation. The apparent strain applied to the overall specimen is usually larger than the real strain in the specimen.

This Perspective deals with possible routes to stretchable semiconductors. Stretchable high-k dielectric materials are also essential in the fabrication of intrinsically stretchable transistors. So far, the electrolyte gels have been the only choice for the stretchable dielectric material.[124−126] The large capacitance is a great advantage of the electrolyte gel. The ions in the electrolyte gels are reported to dope in semiconducting polymers, so the channel shows the electrochemical transistor behavior. Micropatterning of thin electrolyte gels (<100 nm thick) is critical in realization of electrolyte-based transistors.[127] The ion molecules in the ion gel dielectric have sluggish translation under gate potential. This sluggish translation cannot catch up with the switching potential as the frequency increases (f > 100 Hz); hence, the capacitance drops sharply at high frequencies. Thin ion-gel dielectric is expected to reduce this drawback because the switching of the dielectric layer can be instant to the high frequency potential changes. In addition, the electrostatic attraction between the separated charges in a thin ion-gel layer is expected to prevent the diffusion of the ion molecules into the active layer, which can stabilize the performance of the devices for long-term use. Jeong and workers reported the preparation of thin ion gels (h < 100 nm).[127] The thin ion-gel transistors showed excellent gate modulation of the drain current and stable operation at low voltages (−0.3 V). The transistors showed a very small hysteresis during the repeated cycles, which is not usually observed in ion gel gated transistors. Combination of stretchable semiconductors with the ion-gel dielectric can enable immediate fabrication of all-stretchable transistors. However, realization of thin ion gels with a well-defined micropattern is a challenging task because of the rapid dewetting of the gel solution on most substrates. Another way to produce a stretchable dielectric layer is a rubber composite with high-k nanomaterials which have not been reported so far.

AUTHOR INFORMATION

Corresponding Author

*E-mail ujeong@postech.ac.kr (U.J.).

Notes

The authors declare no competing financial interest.

Biographies

Yujeong Lee received a B.S. degree in textile system engineering from Kyungbook National University in 2011. She has been a graduate student in Materials Science and engineering in Yonsei University since 2012. Her current research interests include the control of nanowires produced by the self-assembly of the organic semiconductor polymer and analysis of structural characterization for fabrication of electronic devices.

DOI: 10.1021/acs.macromol.5b02268
Macromolecules 2016, 49, 433−444

Minkwan Shin received a B.S. degree in materials science and engineering from Yonsei University in 2010. He received his Ph.D. in the same department under the guidance of Prof. Unyong Jeong in 2015. His research interests include the design and fabrication of nanocomposite materials for stretchable devices and the control of 1-D polymer nanofibrils to enhance their mechanical properties.

Kaliannan Thiyagarajan received his B.Sc and M.Sc degree in physics from Bharathiar University; he has also done M.Tech in Nanotechnology from Anna University. He received his Ph.D. degree in Mechatronics Engineering from Jeju National University, Republic of Korea. He has done his doctoral thesis in the field of graphene electronics. Currently he is a postdoctoral fellow in professor Unyong Jeong'group and working on the stretchable transistors.

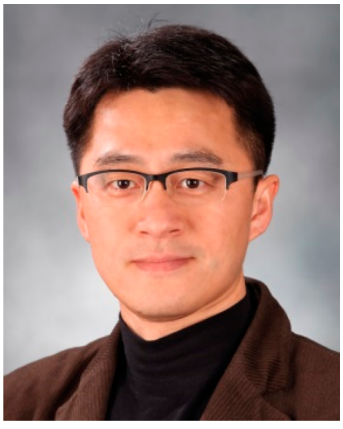

Unyong Jeong received a B.S. degree in chemical engineering from Pohang University of Science and Technology (POSTECH) in Korea (1998). He received a M.A. degree (2000) and a Ph.D. degree (2003) on polymer physics in the same department. He joined Prof. Younan Xia's group as a postdoctoral fellow to study the synthesis and applications of inorganic nanostructured materials. Then, he joined in Yonsei University in Korea (2006) and he moved to Dept. Materials Science and Engineering at POSTECH as an associate professor (2015). His research aims at understanding the mechanical electrical properties of conductive materials and fabricating stretchable electronic devices based on material synthesis, assembly of the materials, and formation of nanocomposites.

■ ACKNOWLEDGMENTS

This work was supported by the Ministry of Science, ICT and Future Planning (MSIP), Korea, under the "IT Consilience Creative Program" (NIPA-2013-H0203-13-1001) supervised by the NIPA.

■ REFERENCES

(1) Lipomi, D. J.; Tee, B. C. K.; Vosgueritchian, M.; Bao, Z. *Adv. Mater.* **2011**, *23* (15), 1771−1775.
(2) Hu, L.; Pasta, M.; Mantia, F. L.; Cui, L.; Jeong, S.; Deshazer, H. D.; Choi, J. W.; Han, S. M.; Cui, Y. *Nano Lett.* **2010**, *10* (2), 708−714.
(3) Gaikwad, A. M.; Zamarayeva, A. M.; Rousseau, J.; Chu, H.; Derin, I.; Steingart, D. A. *Adv. Mater.* **2012**, *24* (37), 5071−5076.
(4) Lipomi, D. J.; Vosgueritchian, M.; Tee, B. C. K.; Hellstrom, S. L.; Lee, J. A.; Fox, C. H.; Bao, Z. *Nat. Nanotechnol.* **2011**, *6* (12), 788−792.
(5) Wang, C.; Hwang, D.; Yu, Z.; Takei, K.; Park, J.; Chen, T.; Ma, B.; Javey, A. *Nat. Mater.* **2013**, *12* (10), 899−904.
(6) Wang, X.; Dong, L.; Zhang, H.; Yu, R.; Pan, C.; Wang, Z. L. *Adv. Sci.* **2015**, *2*, 1500169.
(7) Liang, J.; Li, L.; Niu, X.; Yu, Z.; Pei, Q. *Nat. Photonics* **2013**, *7* (10), 817−824.
(8) Wang, J.; Yan, C.; Chee, K. J.; Lee, P. S. *Adv. Mater.* **2015**, *27* (18), 2876−2882.
(9) Kim, D.-H.; Lu, N.; Ma, R.; Kim, Y.-S.; Kim, R.-H.; Wang, S.; Wu, J.; Won, S. M.; Tao, H.; Islam, A.; Yu, K. J.; Kim, T.-i.; Chowdhury, R.; Ying, M.; Xu, L.; Li, M.; Chung, H.-J.; Keum, H.; McCormick, M.; Liu, P.; Zhang, Y.-W.; Omenetto, F. G.; Huang, Y.; Coleman, T.; Rogers, J. A. *Science* **2011**, *333* (6044), 838−843.
(10) Choong, C.-L.; Shim, M.-B.; Lee, B.-S.; Jeon, S.; Ko, D.-S.; Kang, T.-H.; Bae, J.; Lee, S. H.; Byun, K.-E.; Im, J.; Jeong, Y. J.; Park, C. E.; Park, J.-J.; Chung, U. I. *Adv. Mater.* **2014**, *26* (21), 3451−3458.
(11) Park, J.; Lee, Y.; Hong, J.; Ha, M.; Jung, Y.-D.; Lim, H.; Kim, S. Y.; Ko, H. *ACS Nano* **2014**, *8* (5), 4689−4697.
(12) Jeong, J.-W.; Kim, M. K.; Cheng, H.; Yeo, W.-H.; Huang, X.; Liu, Y.; Zhang, Y.; Huang, Y.; Rogers, J. A. *Adv. Healthcare Mater.* **2014**, *3* (5), 621−621.
(13) Rogers, J. A.; Someya, T.; Huang, Y. *Science* **2010**, *327* (5973), 1603−1607.
(14) Sekitani, T.; Someya, T. *Adv. Mater.* **2010**, *22* (20), 2228−2246.
(15) Yao, S.; Zhu, Y. *Adv. Mater.* **2015**, *27* (9), 1480−1511.
(16) Cheng, T.; Zhang, Y.; Lai, W.-Y.; Huang, W. *Adv. Mater.* **2015**, *27* (22), 3349−3376.
(17) Matsuhisa, N.; Kaltenbrunner, M.; Yokota, T.; Jinno, H.; Kuribara, K.; Sekitani, T.; Someya, T. *Nat. Commun.* **2015**, *6*, 7461.
(18) Menard, E.; Lee, K. J.; Khang, D.-Y.; Nuzzo, R. G.; Rogers, J. A. *Appl. Phys. Lett.* **2004**, *84* (26), 5398−5400.
(19) Choi, W. M.; Song, J.; Khang, D.-Y.; Jiang, H.; Huang, Y. Y.; Rogers, J. A. *Nano Lett.* **2007**, *7* (6), 1655−1663.
(20) Kim, D.-H.; Xiao, J.; Song, J.; Huang, Y.; Rogers, J. A. *Adv. Mater.* **2010**, *22* (19), 2108−2124.
(21) Choi, J.-S.; Na, B. S.; Lim, S. C.; Lee, S. S.; Cho, K.-I.; Chu, H. Y.; Koo, J. B.; Jung, S.-W.; Yoon, S.-M. *IEEE Electron Device Lett.* **2014**, *35* (7), 762−764.
(22) Drack, M.; Graz, I.; Sekitani, T.; Someya, T.; Kaltenbrunner, M.; Bauer, S. *Adv. Mater.* **2015**, *27* (1), 34−40.
(23) Kaltenbrunner, M.; Sekitani, T.; Reeder, J.; Yokota, T.; Kuribara, K.; Tokuhara, T.; Drack, M.; Schwodiauer, R.; Graz, I.; Bauer-Gogonea, S.; Bauer, S.; Someya, T. *Nature* **2013**, *499* (7459), 458−463.
(24) Park, M.; Park, J.; Jeong, U. *Nano Today* **2014**, *9* (2), 244−260.
(25) Park, J.; You, I.; Shin, S.; Jeong, U. *ChemPhysChem* **2015**, *16* (6), 1155−1163.
(26) Kim, K.; Kim, J.; Hyun, B. G.; Ji, S.; Kim, S.-Y.; Kim, S.; An, B. W.; Park, J.-U. *Nanoscale* **2015**, *7* (35), 14577−14594.
(27) Um, D.-S.; Lim, S.; Lee, Y.; Lee, H.; Kim, H.-j.; Yen, W.-C.; Chueh, Y.-L.; Ko, H. *ACS Nano* **2014**, *8* (3), 3080−3087.
(28) Chae, S. H.; Yu, W. J.; Bae, J. J.; Duong, D. L.; Perello, D.; Jeong, H. Y.; Ta, Q. H.; Ly, T. H.; Vu, Q. A.; Yun, M.; Duan, X.; Lee, Y. H. *Nat. Mater.* **2013**, *12* (5), 403−409.
(29) Lee, S.-K.; Kim, B. J.; Jang, H.; Yoon, S. C.; Lee, C.; Hong, B. H.; Rogers, J. A.; Cho, J. H.; Ahn, J.-H. *Nano Lett.* **2011**, *11* (11), 4642−4646.
(30) Castles, F.; Morris, S. M.; Hung, J. M. C.; Qasim, M. M.; Wright, A. D.; Nosheen, S.; Choi, S. S.; Outram, B. I.; Elston, S. J.; Burgess, C.; Hill, L.; Wilkinson, T. D.; Coles, H. J. *Nat. Mater.* **2014**, *13* (8), 817−821.

DOI: 10.1021/acs.macromol.5b02268
Macromolecules 2016, 49, 433−444

(31) Kim, K. S.; Zhao, Y.; Jang, H.; Lee, S. Y.; Kim, J. M.; Kim, K. S.; Ahn, J.-H.; Kim, P.; Choi, J.-Y.; Hong, B. H. *Nature* **2009**, *457* (7230), 706−710.
(32) Pu, J.; Zhang, Y.; Wada, Y.; Tse-Wei Wang, J.; Li, L.-J.; Iwasa, Y.; Takenobu, T. *Appl. Phys. Lett.* **2013**, *103* (2), 023505.
(33) Zang, J.; Ryu, S.; Pugno, N.; Wang, Q.; Tu, Q.; Buehler, M. J.; Zhao, X. *Nat. Mater.* **2013**, *12* (4), 321−325.
(34) Hyun, D. C.; Park, M.; Park, C.; Kim, B.; Xia, Y.; Hur, J. H.; Kim, J. M.; Park, J. J.; Jeong, U. *Adv. Mater.* **2011**, *23* (26), 2946−2950.
(35) Park, M.; Im, J.; Shin, M.; Min, Y.; Park, J.; Cho, H.; Park, S.; Shim, M.-B.; Jeon, S.; Chung, D.-Y.; Bae, J.; Park, J.; Jeong, U.; Kim, K. *Nat. Nanotechnol.* **2012**, *7* (12), 803−809.
(36) Sekitani, T.; Nakajima, H.; Maeda, H.; Fukushima, T.; Aida, T.; Hata, K.; Someya, T. *Nat. Mater.* **2009**, *8* (6), 494−499.
(37) Widlund, T.; Yang, S.; Hsu, Y.-Y.; Lu, N. *Int. J. Solids Struct.* **2014**, *51* (23−24), 4026−4037.
(38) Printz, A. D.; Zaretski, A. D.; Savagatrup, S.; Chiang, A.; Lipomi, D. J. *ACS Appl. Mater. Interfaces* **2015**, *7* (41), 23257−23264.
(39) Khang, D.-Y.; Rogers, J. A.; Lee, H. H. *Adv. Funct. Mater.* **2008**, *18*, 1−11.
(40) Yu, C.; Jiang, H. *Thin Solid Films* **2010**, *519* (2), 818−822.
(41) Khang, D.-Y.; Jiang, H.; Huang, Y.; Rogers, J. A. *Science* **2006**, *311* (5758), 208−212.
(42) Kim, D.-H.; Liu, Z.; Kim, Y.-S.; Wu, J.; Song, J.; Kim, H.-S.; Huang, Y.; Hwang, K.-c.; Zhang, Y.; Rogers, J. A. *Small* **2009**, *5* (24), 2841−2847.
(43) Kim, D.-H.; Ahn, J.-H.; Choi, W. M.; Kim, H.-S.; Kim, T.-H.; Song, J.; Huang, Y. Y.; Liu, Z.; Lu, C.; Rogers, J. A. *Science* **2008**, *320* (5875), 507−511.
(44) Wu, H.; Kustra, S.; Gates, E. M.; Bettinger, C. J. *Org. Electron.* **2013**, *14* (6), 1636−1642.
(45) Kaltenbrunner, M.; White, M. S.; Głowacki, E. D.; Sekitani, T.; Someya, T.; Sariciftci, N. S.; Bauer, S. *Nat. Commun.* **2012**, *3*, 770.
(46) Kim, N.; Kee, S.; Lee, S. H.; Lee, B. H.; Kahng, Y. H.; Jo, Y.-R.; Kim, B.-J.; Lee, K. *Adv. Mater.* **2014**, *26* (14), 2268−2272.
(47) Kinoshita, S.; Yoshioka, S. *ChemPhysChem* **2005**, *6* (8), 1442−1459.
(48) Bowden, N.; Brittain, S.; Evans, A. G.; Hutchinson, J. W.; Whitesides, G. M. *Nature* **1998**, *393* (6681), 146−149.
(49) Hyun, D. C.; Moon, G. D.; Park, C. J.; Kim, B. S.; Xia, Y.; Jeong, U. *Adv. Mater.* **2010**, *22* (24), 2642−2646.
(50) Hyun, D. C.; Moon, G. D.; Park, C. J.; Kim, B. S.; Xia, Y.; Jeong, U. *Angew. Chem., Int. Ed.* **2011**, *50* (3), 724−727.
(51) Zhang, P.; Yang, D.; Li, Z.; Ma, H. *Soft Matter* **2010**, *6* (18), 4580−4584.
(52) Watanabe, M. *J. Appl. Polym. Sci.* **2006**, *101* (3), 2040−2044.
(53) Gray, D. S.; Tien, J.; Chen, C. S. *Adv. Mater.* **2004**, *16* (5), 393−397.
(54) Gonzalez, M.; Axisa, F.; Bulcke, M. V.; Brosteaux, D.; Vandevelde, B.; Vanfleteren, J. *Microelectron. Reliab.* **2008**, *48* (6), 825−832.
(55) Brosteaux, D.; Axisa, F.; Gonzalez, M.; Vanfleteren, J. *IEEE Electron Device Lett.* **2007**, *28* (7), 552−554.
(56) Xu, S.; Zhang, Y.; Cho, J.; Lee, J.; Huang, X.; Jia, L.; Fan, J. A.; Su, Y.; Su, J.; Zhang, H.; Cheng, H.; Lu, B.; Yu, C.; Chuang, C.; Kim, T.-i.; Song, T.; Shigeta, K.; Kang, S.; Dagdeviren, C.; Petrov, I.; Braun, P. V.; Huang, Y.; Paik, U.; Rogers, J. A. *Nat. Commun.* **2013**, *4*, 1543.
(57) Li, M.; Xia, J.; Li, R.; Kang, Z.; Su, Y. *J. Mater. Sci.* **2013**, *48* (24), 8443−8448.
(58) Fan, J. A.; Yeo, W.-H.; Su, Y.; Hattori, Y.; Lee, W.; Jung, S.-Y.; Zhang, Y.; Liu, Z.; Cheng, H.; Falgout, L.; Bajema, M.; Coleman, T.; Gregoire, D.; Larsen, R. J.; Huang, Y.; Rogers, J. A. *Nat. Commun.* **2014**, *5*, 3266.
(59) Shin, M.; Oh, J. Y.; Byun, K.-E.; Lee, Y.-J.; Kim, B.; Baik, H.-K.; Park, J.-J.; Jeong, U. *Adv. Mater.* **2015**, *27* (7), 1255−1261.
(60) Xie, X.; Sakkar, D.; Liu, W.; Kang, J.; Marinov, O.; Deen, M. J.; Banerjee, K. *ACS Nano* **2014**, *8* (6), 5633−5640.
(61) Dadlani, A. L.; Trejo, O.; Acharya, S.; Torgersen, J.; Petousis, I.; Nordlund, D.; Sarangi, R.; Schindler, P.; Prinz, F. B. *J. Mater. Chem. C* **2015**, *3*, 12192.
(62) Wang, X.; Gong, Y.; Shi, G.; Leong, W.; Keyshar, K.; Ye, G.; Vajtai, R.; Lou, J.; Liu, Z.; Ringe, E.; Tay, B. K.; Ajayan, P. M. *ACS Nano* **2014**, *8* (5), 5125−5131.
(63) Mak, K. F.; McGill, K. L.; Park, J.; McEuen, P. L. *Science* **2014**, *344* (6191), 1489−1492.
(64) Holten-Andersen, N.; Harrington, M. J.; Birkedal, H.; Lee, B. P.; Messersmith, P. B.; Lee, K. Y. C.; Waite, J. H. *Proc. Natl. Acad. Sci. U. S. A.* **2011**, *108* (7), 2651−2655.
(65) Xie, B.; Liu, Y.; Ding, Y.; Zheng, Q.; Xu, Z. *Soft Matter* **2011**, *7* (21), 10039−10047.
(66) Wang, C.; Xie, B.; Liu, Y.; Xu, Z. *ACS Macro Lett.* **2012**, *1* (10), 1176−1179.
(67) Qian, D.; Dickey, E. C.; Andrews, R.; Rantell, T. *Appl. Phys. Lett.* **2000**, *76* (20), 2868−2870.
(68) Qian, D.; Liu, W. K.; Ruoff, R. S. *Compos. Sci. Technol.* **2003**, *63* (11), 1561−1569.
(69) Xu, M.; Futaba, D. N.; Yamada, T.; Yumura, M.; Hata, K. *Science* **2010**, *330* (6009), 1364−1368.
(70) Chen, Y.; Pan, F.; Guo, Z.; Liu, B.; Zhang, J. *J. Mech. Phys. Solids* **2015**, *84*, 395−423.
(71) Akter, T.; Kim, W. S. *ACS Appl. Mater. Interfaces* **2012**, *4* (4), 1855−1859.
(72) Kim, J.; Lee, M.-S.; Jeon, S.; Kim, M.; Kim, S.; Kim, K.; Bien, F.; Hong, S. Y.; Park, J.-U. *Adv. Mater.* **2015**, *27* (21), 3292−3297.
(73) Oh, J. Y.; Shin, M.; Lee, T. I.; Jang, W. S.; Lee, Y.-J.; Kim, C. S.; Kang, J.-W.; Myoung, J.-M.; Baik, H. K.; Jeong, U. *Macromolecules* **2013**, *46* (9), 3534−3543.
(74) Vashishth, D.; Tanner, K. E.; Bonfield, W. *J. Biomech* **2003**, *36* (1), 121−124.
(75) Lacour, S. P.; Chan, D.; Wagner, S.; Li, T.; Suo, Z. *Appl. Phys. Lett.* **2006**, *88* (20), 204103.
(76) Graz, I. M.; Cotton, D. P. J.; Lacour, S. P. *Appl. Phys. Lett.* **2009**, *94* (7), 071902.
(77) Yamada, T.; Hayamizu, Y.; Yamamoto, Y.; Yomogida, Y.; Izadi-Najafabadi, A.; Futaba, D. N.; Hata, K. *Nat. Nanotechnol.* **2011**, *6* (5), 296−301.
(78) Graudejus, O.; Morrison, B.; Goletiani, C.; Yu, Z.; Wagner, S. *Adv. Funct. Mater.* **2012**, *22* (3), 640−651.
(79) Gutruf, P.; M Shah, C.; Walia, S.; Nili, H.; S Zoolfakar, A.; Karnutsch, C.; Kalantar-zadeh, K.; Sriram, S.; Bhaskaran, M. *NPG Asia Mater.* **2013**, *5*, e62.
(80) Savagatrup, S.; Printz, A. D.; O'Connor, T. F.; Zaretski, A. V.; Rodriquez, D.; Sawyer, E. J.; Rajan, K. M.; Acosta, R. I.; Root, S. E.; Lipomi, D. J. *Energy Environ. Sci.* **2015**, *8* (1), 55−80.
(81) Chortos, A.; Lim, J.; To, J. W. F.; Vosgueritchian, M.; Dusseault, T. J.; Kim, T.-H.; Hwang, S.; Bao, Z. *Adv. Mater.* **2014**, *26* (25), 4253−4259.
(82) Lu, N.; Wang, X.; Suo, Z.; Vlassak, J. *Appl. Phys. Lett.* **2007**, *91* (22), 221909.
(83) O'Connor, B.; Kline, R. J.; Conrad, B. R.; Richter, L. J.; Gundlach, D.; Toney, M. F.; DeLongchamp, D. M. *Adv. Funct. Mater.* **2011**, *21* (19), 3697−3705.
(84) Yasuda, T. *Phys. Status Solidi C* **2011**, *8* (2), 604−606.
(85) Sekitani, T.; Kato, Y.; Iba, S.; Shinaoka, H.; Someya, T.; Sakurai, T.; Takagi, S. *Appl. Phys. Lett.* **2005**, *86* (7), 073511.
(86) Tahk, D.; Lee, H. H.; Khang, D.-Y. *Macromolecules* **2009**, *42* (18), 7079−7083.
(87) Lipomi, D. J.; Bao, Z. *Energy Environ. Sci.* **2011**, *4* (9), 3314−3328.
(88) Savagatrup, S.; Printz, A. D.; Rodriquez, D.; Lipomi, D. J. *Macromolecules* **2014**, *47* (6), 1981−1992.
(89) O'Connor, B.; Chan, E. P.; Chan, C.; Conrad, B. R.; Richter, L. J.; Kline, R. J.; Heeney, M.; McCulloch, I.; Soles, C. L.; DeLongchamp, D. M. *ACS Nano* **2010**, *4* (12), 7538−7544.
(90) Awartani, O.; Lemanski, B. I.; Ro, H. W.; Richter, L. J.; DeLongchamp, D. M.; O'Connor, B. T. *Adv. Energy Mater.* **2013**, *3* (3), 399−406.
(91) Savagatrup, S.; Makaram, A. S.; Burke, D. J.; Lipomi, D. J. *Adv. Funct. Mater.* **2014**, *24* (8), 1169−1181.

DOI: 10.1021/acs.macromol.5b02268
Macromolecules 2016, 49, 433−444

(92) Kim, J. Y.; Frisbie, C. D. *J. Phys. Chem. C* **2008**, *112* (45), 17726−17736.
(93) Zhao, J.; Swinnen, A.; Van Assche, G.; Manca, J.; Vanderzande, D.; Mele, B. V. *J. Phys. Chem. B* **2009**, *113* (6), 1587−1591.
(94) Seitz, J. T. *J. Appl. Polym. Sci.* **1993**, *49* (8), 1331−1351.
(95) Fedors, R. F. *Polym. Eng. Sci.* **1974**, *14* (2), 147−154.
(96) Savagatrup, S.; Printz, A. D.; Wu, H.; Rajan, K. M.; Sawyer, E. J.; Zaretski, A. V.; Bettinger, C. J.; Lipomi, D. J. *Synth. Met.* **2015**, *203*, 208−214.
(97) Kim, T.; Kim, J. H.; Kang, T. E.; Lee, C.; Kang, H.; Shin, M.; Wang, C.; Ma, B.; Jeong, U.; Kim, T. S.; Kim, B. J. *Nat. Commun.* **2015**, *6* (Oct.9), 8547.
(98) Peng, R.; Pang, B.; Hu, D.; Chen, M.; Zhang, G.; Wang, X.; Lu, H.; Cho, K.; Qiu, L. *J. Mater. Chem. C* **2015**, *3* (15), 3599−3606.
(99) Jacobsen, S.; Fritz, H. G. *Polym. Eng. Sci.* **1999**, *39* (7), 1303−1310.
(100) Baiardo, M.; Frisoni, G.; Scandola, M.; Rimelen, M.; Lips, D.; Ruffieux, K.; Wintermantel, E. *J. Appl. Polym. Sci.* **2003**, *90* (7), 1731−1738.
(101) Fox, T. G. *Bull. Am. Chem. Phys. Soc.* **1956**, *1*, 123.
(102) Crispin, X.; Jakobsson, F. L. E.; Crispin, A.; Grim, P. C. M.; Andersson, P.; Volodin, A.; van Haesendonck, C.; Van der Auweraer, M.; Salaneck, W. R.; Berggren, M. *Chem. Mater.* **2006**, *18* (18), 4354−4360.
(103) Hecht, D. S.; Hu, L.; Irvin, G. *Adv. Mater.* **2011**, *23* (13), 1482−1513.
(104) Vosgueritchian, M.; Lipomi, D. J.; Bao, Z. *Adv. Funct. Mater.* **2012**, *22* (2), 421−428.
(105) Oh, J. Y.; Shin, M.; Lee, J. B.; Ahn, J.-H.; Baik, H. K.; Jeong, U. *ACS Appl. Mater. Interfaces* **2014**, *6* (9), 6954−6961.
(106) Lindell, L.; Burquel, A.; Jakobsson, F. L. E.; Lemaur, V.; Berggren, M.; Lazzaroni, R.; Cornil, J.; Salaneck, W. R.; Crispin, X. *Chem. Mater.* **2006**, *18* (18), 4246−4252.
(107) Zhou, Y.; Fuentes-Hernandez, C.; Shim, J.; Meyer, J.; Giordano, A. J.; Li, H.; Winget, P.; Papadopoulos, T.; Cheun, H.; Kim, J.; Fenoll, M.; Dindar, A.; Haske, W.; Najafabadi, E.; Khan, T. M.; Sojoudi, H.; Barlow, S.; Graham, S.; Brédas, J.-L.; Marder, S. R.; Kahn, A.; Kippelen, B. *Science* **2012**, *336* (6079), 327−332.
(108) Oh, J. Y.; Kim, S.; Baik, H. K.; Jeong, U. *Adv. Mater.* **2015**, DOI: 10.1002/adma.201502947.
(109) Savagatrup, S.; Printz, A. D.; O'Connor, T. F.; Zaretski, A. V.; Lipomi, D. J. *Chem. Mater.* **2014**, *26* (10), 3028−3041.
(110) Lee, S.; Moon, G. D.; Jeong, U. *J. Mater. Chem.* **2009**, *19* (6), 743−748.
(111) Min, S.-Y.; Kim, T.-S.; Lee, Y.; Cho, H.; Xu, W.; Lee, T.-W. *Small* **2015**, *11* (1), 45−62.
(112) Chou, C.-C.; Wu, H.-C.; Lin, C.-J.; Ghelichkhani, E.; Chen, W.-C. *Macromol. Chem. Phys.* **2013**, *214* (7), 751−760.
(113) Takayanagi, M.; Uemura, S.; Minami, S. *J. Polym. Sci., Part C: Polym. Symp.* **1964**, *5* (1), 113−122.
(114) Ji, X. L.; Jing, J. K.; Jiang, W.; Jiang, B. Z. *Polym. Eng. Sci.* **2002**, *42* (5), 983−993.
(115) Gray, R. W.; McCrum, N. G. *J. Polym. Sci.* **1969**, *7* (8), 1329−1355.
(116) Oh, J. Y.; Lee, T. I.; Myoung, J.-M.; Biak, H. K.; Jeong, U. *Macromol. Rapid Commun.* **2011**, *32* (14), 1066−1071.
(117) Oh, J. Y.; Shin, M.; Lee, T. I.; Jang, W. S.; Min, Y.; Myoung, J.-M.; Biak, H. K.; Jeong, U. *Macromolecules* **2012**, *45* (18), 7504−7513.
(118) Oh, J. Y.; Shin, M.; Lee, T. I.; Jang, W. S.; Lee, Y.-J.; Kim, C. S.; Kang, J.-W.; Myoung, J.-M.; Biak, H. K.; Jeong, U. *Macromolecules* **2013**, *46* (9), 3534−3543.
(119) Nam, K. H.; Park, I. H.; Ko, S. H. *Nature* **2012**, *485* (7397), 221−224.
(120) Kang, D.; Pikhitsa, V.; Choi, Y. W.; Lee, C.; Shin, S. S.; Piao, L.; Park, B.; Suh, K.-Y.; Kim, T.-I.; Choi, M. *Nature* **2014**, *516* (7530), 222−226.
(121) Cui, L.; Ranade, A.; Matos, M. A.; Dubois, G.; Dauskardt, R. H. *ACS Appl. Mater. Interfaces* **2013**, *5* (17), 8495−8504.
(122) Cui, L.; Lionti, K.; Ranade, A.; Larson-Smith, K.; Dubois, G.; Dauskardt, R. H. *ACS Nano* **2014**, *8* (7), 7186−7191.
(123) Dupont, S. R.; Novoa, F.; Voroshaz, E.; Dauskardt, R. H. *Adv. Funct. Mater.* **2014**, *24* (9), 1325−1332.
(124) Lee, S. W.; Lee, H. J.; Choi, J. H.; Koh, W. G.; Myoung, J. M.; Hur, J. H.; Park, J. J.; Cho, J. H.; Jeong, U. *Nano Lett.* **2010**, *10* (1), 347−351.
(125) Kim, B. J.; Jang, H.; Lee, S.-K.; Hong, B. H.; Ahn, J.-H.; Cho, J. H. *Nano Lett.* **2010**, *10* (9), 3464−3466.
(126) Kim, S. H.; Hong, K.; Xie, W.; Lee, K. H.; Zhang, S.; Lodge, T. P.; Frisbie, C. D. *Adv. Mater.* **2013**, *25* (13), 1822−1846.
(127) Lee, S. W.; Shin, M. K.; Park, J.; Kim, B.; Tu, D.; Jeon, S.; Jeong, U. *Sci. Adv. Mater.* **2015**, *7* (5), 874−880.

DOI: 10.1021/acs.macromol.5b02268
Macromolecules 2016, 49, 433−444